Continental Shelf Research 135 (2017) 23–34

Contents lists available at ScienceDirect

Continental Shelf Research

journal homepage: www.elsevier.com/locate/csr

Research papers

Methane in the South China Sea and the Western Philippine Sea

Hsiao-Chun Tseng[a,b], Chen-Tung Arthur Chen[b,*], Alberto V. Borges[c], T. Angel DelValls[a], Yu-Chang Chang[b]

[a] UNESCO UNITWIN/WiCop. Physical Chemistry Department. Faculty of Marine and Environmental Sciences, Polígono río San Pedro s/n, University of Cadiz, 11519, Puerto Real, Cadiz, Spain
[b] Department of Oceanography, National Sun Yat-sen University, Kaohsiung 804, Taiwan
[c] Université de Liège, Unité d'Océanographie Chimique, Institut de Physique (B5), B-4000, Belgium

ARTICLE INFO

Keywords:
South China Sea
Western Philippine Sea
CH_4
Sea-to-air flux
Chlorophyll *a*
Gas hydrates

ABSTRACT

Approximately 700 water samples from the South China Sea (SCS) and 300 water samples from the western Philippine Sea (wPS) were collected during eight cruises from August 2003 to July 2007 to determine methane (CH_4) distributions from the surface to a depth of 4250 m. The surface CH_4 concentrations exceeded atmospheric equilibrium, both in the SCS and the wPS, and the concentrations were 4.5 ± 3.6 and 3.0 ± 1.2 nmol L^{-1}, respectively. The sea-to-air fluxes were calculated, and the SCS and the wPS were found to emit CH_4 to the atmosphere at 8.6 ± 6.4 μmol m^{-2} d^{-1} and 4.9 ± 4.9 μmol m^{-2} d^{-1}, respectively. In the SCS, CH_4 emissions were higher over the continental shelf (11.0 ± 7.4 μmol m^{-2} d^{-1}) than over the deep ocean (6.1 ± 6.0 μmol m^{-2} d^{-1}), owing to greater biological productivity and closer coupling with the sediments on the continental shelf. The SCS emitted 30.1×10^6 mol d^{-1} CH_4 to the atmosphere and exported 1.82×10^6 mol d^{-1} CH_4 to the wPS.

The concentrations of both CH_4 and chlorophyll *a* were high in the 150 m surface layer of the wPS, but were not significantly correlated with each other. CH_4 concentrations generally declined with increasing depth below the euphotic zone but remained constant below 1,000 m, both in the SCS and the wPS. Some high CH_4 concentrations were observed at mid-depths and bottom waters in the SCS, and were most likely caused by the release of CH_4 from gas hydrates or gas seepage.

1. Introduction

Methane (CH_4), the most abundant hydrocarbon in the atmosphere, has a global warming potential in a 100-year time frame (GWP_{100}) that is 34 times that of carbon dioxide (CO_2), and plays an important role in the atmospheric chemistry (Naqvi et al., 2010; IPCC, 2013).

The global atmospheric concentration of CH_4 has increased exponentially from a pre-industrial value of about 722 ± 25 ppb in 1750 to 1803 ± 2 ppb in 2011 (IPCC, 2013). This increase in CH_4 concentration is very likely caused by anthropogenic activities, predominantly agriculture and combustion of fossil fuels, but the relative contributions of different sources have not been well determined (IPCC, 2013). Kirschke et al. (2013) stated that the surface-to-air global CH_4 emission from 2000 to 2009 was 678 Tg CH_4 yr^{-1}, with a large range (542–852 Tg CH_4 yr^{-1}). The ocean emits CH_4 to the atmosphere at a rate of less than 2 Tg CH_4 yr^{-1} (Rhee et al., 2009) and its contribution to the atmospheric CH_4 budget is minor (around 2%). However, the impingement of human activities on oceanic CH_4 emissions, such as waste water discharge into the coastal areas, unlike on terrestrial emissions, is not well understood and has been poorly quantified (Naqvi et al., 2010). Especially, continental shelves and estuaries contribute approximately 75% of global oceanic CH_4 emissions (Bange et al., 1994), and CH_4 emissions from these environments are probably higher due to the contribution from sedimentary sources in well-mixed coastal zones (Borges et al., 2016).

The oversaturation of CH_4 in the oxygenated ocean surface mixed layer has been widely known for more than four decades (Lamontagne et al., 1973; Scranton and Brewer, 1977; Forster et al., 2008). The CH_4 concentrations in near-surface waters throughout much of the world's oceans are 5–75% oversaturated with respect to the atmospheric equilibrium (Karl et al., 2008). Previous research has revealed that CH_4 is released during zooplankton grazing (de Angelis and Lee, 1994) or is formed in anoxic microenvironments within zooplankton fecal pellets (Traganza et al., 1979; de Angelis and Lee, 1994; Karl and Tilbrook, 1994), which are mostly found in the euphotic zone. Recent

* Corresponding author.
E-mail address: ctchen@mail.nsysu.edu.tw (C.-T.A. Chen).

http://dx.doi.org/10.1016/j.csr.2017.01.005
Received 19 February 2016; Received in revised form 12 January 2017; Accepted 12 January 2017
Available online 18 January 2017

research has also determined that the formation of CH_4 in oxic environments can occur via methylphosphonate cycling in subtropical gyres, which are phosphate-depleted (Karl et al., 2008), and by dimethylsulfide (DMS) cycling in both polar and tropical oligotrophic waters (Damm et al., 2010; Zindler et al., 2013). Florez-Leiva et al. (2013) suggested that the CH_4 production may be induced by DMS cycling in the surface water of an upwelling ecosystem off central Chile in which nutrient depletion has never been observed even in winter (Morales and Anabalón, 2012). Overall, the enhancement of primary production may lead to increased CH_4 concentrations, which has led Bogart et al. (2014) to suggest the possibility of a relationship between CH_4 concentration and phytoplankton standing stocks (i. e. chlorophyll *a*).

Only recently has CH_4 in the South China Sea (SCS) and the western Philippine Sea (wPS) been studied and the focus has usually been on the surface water (Chen et al., 1994; Rehder and Suess, 2001), the bottom water and sediments (Chuang et al., 2006; Yang et al., 2006). Chen and Tseng (2006), Chen et al. (2008a, 2008b) and Zhou et al. (2009) reported the CH_4 distribution in the water column of the SCS but the study was only local. Here, for the first time we investigated the CH_4 distribution throughout the SCS and the wPS. Our results elucidate the spatial and vertical distributions of CH_4 in the water column of the SCS and wPS, as well as its sea-to-air fluxes. Further, we discuss differences between these seas and factors that influence the distribution and fluxes of CH_4.

2. Materials and methods

2.1. Study area

The SCS is a semi-enclosed marginal sea off the Asian continent in the West Pacific. It is the largest marginal sea in the world with an area of 3.5×10^6 km^2 and an average depth of 1350 m. The SCS properly characterized by either a tropical or subtropical climate has both deep basin and extensive shelf systems at its northern and southern boundaries, which are associated with large riverine inputs. At the southern edge of the SCS lies the Sunda Shelf, which connects the sea to the Straits of Malacca and has an average depth of approximately 50 m. The eastern part of the SCS is connected with the Sulu Sea through the Mindoro Strait, and the northern part of the SCS is connected with the East China Sea through the Taiwan Strait. The northeastern SCS is connected with the wPS via the Luzon Strait, which is around 2200 m in depth and has the deepest sill that connects the SCS with any adjacent body of water. The SCS also features dynamic exchange with the wPS via an upper water exchanges with the Kuroshio and inflow at depth (Chen et al., 2001; Dai et al., 2013; Du et al., 2013).

The Asian monsoon dominates climatic variations at the sea–air interface of the SCS. The southwest monsoon season runs from May to October and brings a large amount of rainfall. The northeast monsoon season runs from November to April and is characterized by the high wind speeds (Han, 1998).

The wPS is located in the western part of the North Pacific from 123°E to 135°E and from 10°N to 35°N. The mean depth of the wPS is about 5500 m. This study focuses on the area between 120.5°E and 130°E and between 21°N and 28°N, where the wPS connects with the SCS and water masses exchange frequently.

2.2. Water samples collections

Samples were taken during six cruises on board R/V Ocean Researchers I and III in the SCS (Fig. 1a; Table 1): ORIII-896 (August, 2003), ORI-695 (September, 2003), ORIII-983 (July, 2004), ORIII-1081 (July, 2005), ORI-802 (July, 2006) and ORI-837 (July, 2007).

In this study, four contrasting physical–biogeochemical domains (Table 1) are examined to provide a better understanding of the spatial variability of CH_4 distributions and fluxes in the SCS. Domain A is in the northeastern part of the SCS, close to the south of the Taiwan Strait. Samples were collected in domain A during the ORIII-896 and ORIII-983 cruises in August 2003 and July 2004, respectively. This area is affected by Kuroshio intrusions, which generate various mesoscale eddies, upwelling and internal waves (Yuan et al., 2008; Sheu et al., 2010; Chen et al., 2015; Huang et al., 2015). Cruises ORI-695 and ORIII-1081 were conducted in September 2003 and July 2005, respectively in domain B in the wet season when the Pearl River exhibited a large discharge (Chen et al., 2008a; Gan et al., 2009; Cao et al., 2011; Han et al., 2012). The Pearl River (Zhujiang) is the second largest river (after the Mekong River) that enters the SCS (Chen et al., 2008a). Domain C is located in the southwestern part of the SCS. In July 2006, samples were taken during the ORI-802 cruise from domain C and time-series station SCS1, which was located in domain B. Some sampling stations were on the Sunda Shelf and others were off the Sunda Shelf and on the continental slope, where the depth increases sharply. Domain D is located from the eastern part to the southern part of the SCS. The samples in domain D were taken during July 16–31 of 2007 during the ORI-837 cruise. Surface water samples were taken from the Luzon Strait and along the western coast of Luzon Island, Palawan Island and northwestern coast of Borneo Island. Discrete water samples were taken at various depths from the eastern part of the SCS to the southern part of the SCS.

Samples from the wPS were collected during three cruises (Fig. 1b). Discrete water samples were taken at various depths on ORI-725 (July, 2004) and ORIII-1149 (May, 2006). These two cruises were carried out along 22°N from 121°E to126°E in July 2004 and from 121°E to124°E in May 2006. Surface water samples were taken from the northeastern coast of Taiwan to the Luzon Strait on ORI-837 (July, 2007). The analysis herein also included a very limited CH_4 data-set which was obtained from 25 samples from surface waters collected exclusively in the wPS in various cruises in the years 1992–1996.

Water samples from various areas and depths were collected using a Rosette sampler that was fitted with 5 L or 10 L Niskin bottles, along with a conductivity–temperature–depth (CTD) probe (Sea-Bird 911, USA). Saturated $HgCl_2$ was added to all samples to inhibit microbial activity, except for those samples that were used to measure salinity. Temperature data were obtained from the CTD profiles, whereas the salinity values that were used in the analysis were determined from discrete AUTOSAL measurements.

Water samples for measuring CH_4 concentration were collected in 120 mL dark glass bottles. The bottles were rinsed three times with the sampled water. After 1–2 fold of bottle volume was allowed to overflow the bottle, 10 mL of the water sample was withdrawn from the bottle to create an air space, and 0.5 mL saturated $HgCl_2$ was then added. The sample bottles were then immediately sealed with a butyl rubber stopper and an aluminum cap. The samples were stored at 4 °C in the dark. All the water samples were transferred to a laboratory and analyzed within three months of collection.

2.3. Atmospheric air samples collections

Atmospheric CH_4 samples were collected using modified version of the sampling method of Chang and Yang (1997). A 12 mL disposable plastic syringe with an 8 cm-long plastic tube was used to withdraw 12 mL of air four times from a 12 mL serum bottle to increase the exchange of the atmospheric gas into the 12 mL serum bottle. The serum bottle was then sealed with a butyl rubber stopper and an aluminum cap. While making CTD casting, gas samples were taken on the top deck to collect clean air, facing into the wind to prevent contamination by the emissions of the ship.

2.4. Chemical analysis

The salinity of the discrete samples was determined by measuring

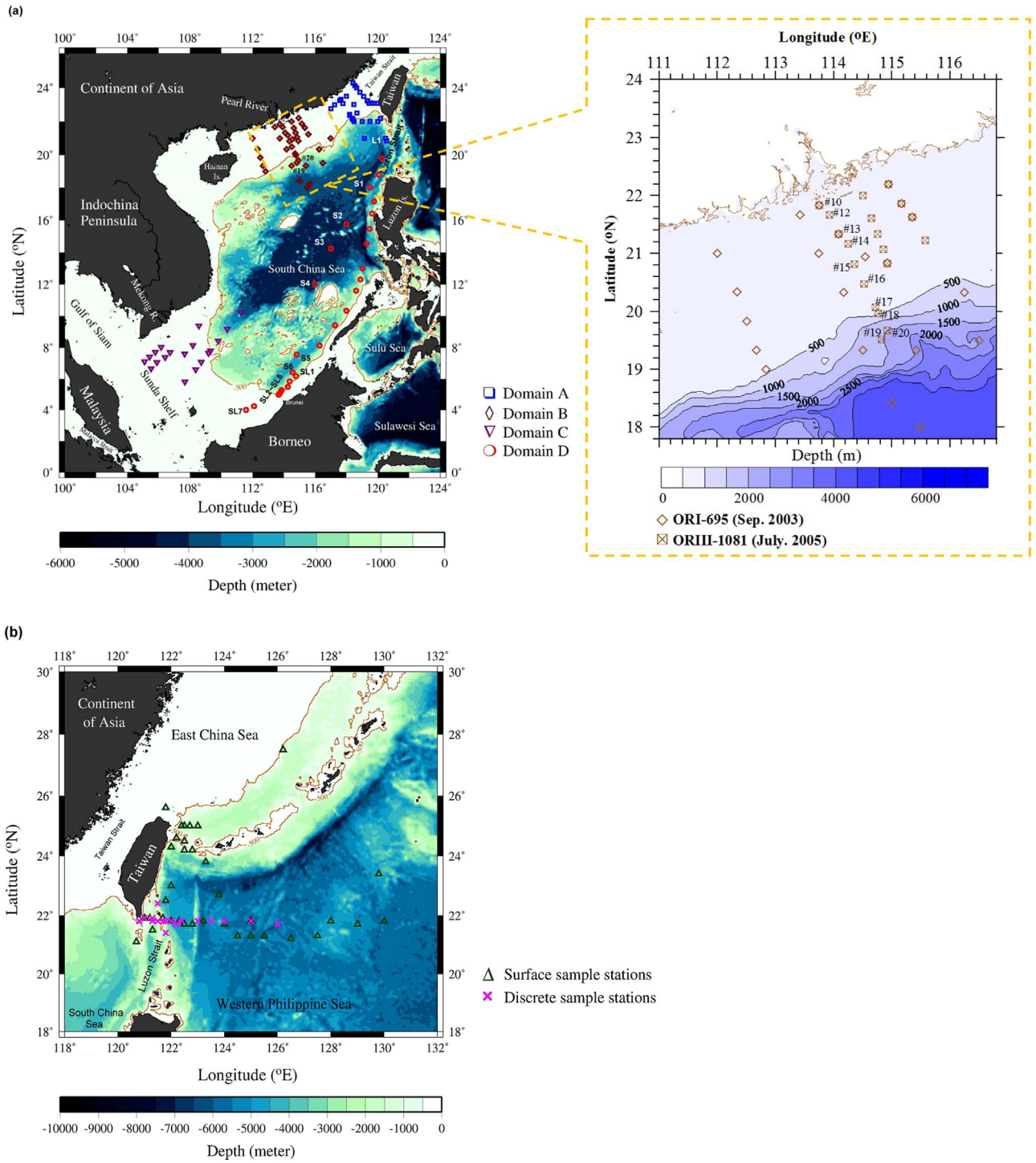

Fig. 1. Study area and station locations: a. South China Sea stations. □: Domain A, ORIII-896 (Aug. 2003) and ORIII-983 (Jul. 2004); ◇: Domain B, ORI-695 (Sep. 2003), ORIII-1081 (Jul. 2005) and ORI-802 (Jul. 2006)-Stn.SCS1; ∇: Domain C, ORI-802 (Jul. 2006); ○: Domain D, ORI-837 (Jul. 2007)); b. Western Philippine Sea stations. Δ: surface sampling stations, ORI-725 (Jul. 2004), ORI-837 (Jul. 2007) -Stn.A-D;1–5 and unpublished data from C. T. A. Chen; ×: discrete sampling stations, ORI-725 (Jul. 2004) and ORIII-1149 (May 2006)).

conductivity using an AUTOSAL salinometer, which was calibrated with standard seawater (batch no. P141) from the International Association for the Physical Sciences of the Oceans (IAPSO). The precision of the measurements was ± 0.003 salinity unit. Chlorophyll *a* samples were collected by filtration through a 0.45 μm diameter Millipore polycarbonate filter. A Turner Designs model 10-AU fluorometer (Varian Eclipse) was utilized to measure chlorophyll *a* concentration following extraction by 90% acetone (Strickland and Parsons, 1972) with a precision of ± 5%.

The concentration of dissolved CH_4 was estimated by the modified head-space equilibrium method (Johnson et al., 1990) using a gas chromatograph (GC; HP 5890 Series II) that was equipped with a flame ionization detector (FID). The samples were placed in a water bath at a constant temperature of 25 °C, and allowed to equilibrate for at least three hours. Finally, 2 mL of the gas from the headspace was injected into the GC. The GC-FID had a 6 foot-long stainless steel column with a diameter of one-eighth of an inch, which was filled with a 60/80 mesh molecular sieve 5 A. The primary standard was NIST (National Institute of Standards and Technology) 1 ppm V CH_4 standard. Mixtures of CH_4 in N_2 at concentrations of 0 (Jing-Shang, Taiwan), 1

Table 1
Surface CH_4 concentrations and sea-to-air fluxes in the SCS and the wPS in the wet season.

			Latitude (°N)	Longitude (°E)	Sal.	Average Surface CH_4 Concentration (nmol L^{-1})	Wind Speed (m/s)	Sea-to-Air Flux (μmol m^{-2} d^{-1})	Surveying Cruises/Months
SCS	Domain	A	20–25	117–120	33.86 ± 0.34	4.5 ± 2.3 (n=31)	7.2 ± 1.8	9.9 ± 8.7	ORIII-896 (Aug. 2003) ORIII-983 (Jul. 2004)
		B	17–23	112–117	33.17 ± 1.08	5.2 ± 2.1 (n=42)	7.0 ± 1.3	12.0 ± 7.4	ORI-695 (Sep. 2003) ORIII-1081 (Jul. 2005) ORI-802 (Jul. 2006)-Stn. SCS1
		C	3–12	104–113	33.23 ± 0.19	4.9 ± 1.5 (n=19)	6.2 ± 1.0	8.3 ± 4.1	ORI-802 (Jul. 2006)
		D	4–20	110–120	32.87 ± 1.00	3.4 ± 1.0 (n=30)	6.3 ± 0.9	4.3 ± 3.9	ORI-837 (Jul. 2007)
	Avg.		3–25	104–120	33.28 ± 1.5	4.5 ± 3.6 (n=122)	6.3 ± 0.8	8.6 ± 6.4	
	Avg. Continental Shelf and upper slope region (depth < 500 m)				33.29 ± 0.9	5.1 ± 2.1 (n=72)		11.0 ± 7.4	
	Avg. Deep Sea (depth > 500 m)				33.54 ± 0.7	3.8 ± 1.6 (n=50)		6.1 ± 6.0	
wPS	Avg		21–26	120.5–130	34.22 ± 0.27	3.0 ± 1.2 (n=68)	7.4 ± 1.3	4.9 ± 4.9	ORI-725 (Jul. 2004) ORIII-1149 (May 2006) ORI-837 (Jul. 2007)-Stn.A-D;1-5, unpublished data from C. T. A. Chen

(NIST, U.S.A), 4.97 (San-Ying, Taiwan), 9.77 (Lien-Hwa, Taiwan) and 53 (All-Win, Taiwan) ppmV were used for calibration. The precision of repeated analysis of water samples was about ± 5% in routine sample analysis.

The concentration of the atmospheric CH_4 was estimated by the GC-FID. Atmospheric CH_4 samples were placed at the room temperature (25 °C) for more than 2 h and 2 mL of the gas in the serum bottle was injected into the GC to analyze the CH_4 concentration. The precision of repeated analysis of air samples was about ± 3% in routine sample analysis.

2.5. Saturation ratio

The concentrations of the CH_4 in the water samples were obtained from the concentrations that were measured in the headspace by subtracting the influence of atmospheric CH_4 at the sampling sites and using the Bunsen coefficients to calculate the equilibrium solubility, which were described in Wiesenburg and Guinasso (1979).

Saturation, expressed in %, was calculated using $R=(C_{obs}/C_{eq})*100$ where C_{obs} represents the observed concentration of gas dissolved in the water, and C_{eq} is the expected equilibrium water concentration.

2.6. Fluxes

Fluxes of CH_4 across the air-water interface were estimated using $F=k(C_w-\beta C_a)$ where k (cm h^{-1}) is the gas exchange coefficient, C_w is the concentration of dissolved gas in the water (mol l^{-1}), β is the Bunsen solubility, and C_a is the atmospheric gas concentration. A positive flux indicates gas transfer from the water to the atmosphere. The value of k is a specific function of properties of the gas, the temperature T (°C) and turbulence, and is frequently parameterized as a function of the wind speed u (m s^{-1}). Many equations are used for calculating the k/wind speed relationship (Liss and Merlivat, 1986; Wanninkhof, 1992; Erickson, 1993; Nightingale et al., 2000). As Wanninkhof (1992) has been widely used and has recently been updated (Wanninkhof, 2014), here, we calculated k by using the relationship established by Wanninkhof (2014). The updated relationship is expressed as $k=0.251u^2(Sc/660)^{-0.5}$, where k is the gas transfer velocity, u^2 is the average squared wind speed, and Sc is the Schmidt number, which is the kinematic viscosity of water divided by the molecular diffusion coefficient of the gas. The new estimates of the Schmidt number (Wanninkhof, 2014) are provided, expanding the temperature range from 0 to 30 °C to −2 to 40 °C. Wind speeds at 10 m above the surface were obtained from the National Aeronautics and Space Administration (NASA) QuikSCAT satellite platform (https://winds.jpl.nasa.gov/missions/quikscat/). The average monthly wind speed was used to estimate the sea-to-air flux.

The seawater fluxes from the SCS to the wPS were calculated as described by Chen et al. (2001). The principle of conservation of water mass dictates that the water flowing into the SCS must be balanced by the water flowing out plus the water piled up within the SCS.

3. Result and discussion

3.1. Atmospheric CH_4 concentration

The mean concentrations of CH_4 in all atmospheric samples from the SCS and wPS were 1.81 ± 0.04 ppm V and 1.82 ± 0.04 ppmV, respectively. These values agreed closely with the mean monthly CH_4 mixing ratios that were measured at stations of the Earth System Research Laboratory under the National Oceanic and Atmospheric Administration (NOAA-ESRL; http://www.esrl.noaa.gov/gmd/ccgg/ggrn.php) in situ program. The mean CH_4 mixing ratios at Station BKT (Bukit Kototabang; 0°12'S, 100°19'E), Station GMI (Mariana Islands; 13°23'N, 144°39'E) and Station MID (Sand Island; 28°12'N, 177°22'E) of NOAA-ESRL between 2003 and 2007 were 1.807 ppm V (1.805–1.809 ppm V), 1.785 ppm V (1.777–1.798 ppm V) and 1.821 ppm V (1.817–1.827 ppm V), respectively.

3.2. Surface seawater CH_4 concentrations and sea-to-air CH_4 fluxes

The average surface CH_4 concentration in the wPS was 3.0 ± 1.2 nmol L^{-1} (155% saturation). This value is greater than the 109% saturation that was reported by Rehder and Suess (2001) in the Pacific Ocean, east of Taiwan, and is also greater than that in the western North Pacific of 2.46 ± 0.23 nmol L^{-1} (saturation 132%) in 1991 (Watanabe et al., 1995) and 1.83–2.81 nmol L^{-1} in 1979 (Burke et al., 1983). In addition to the fact that the concentration of CH_4 at the surface may increase in parallel with the atmospheric concentration (Watanabe et al., 1995), the surface water in the wPS is influenced by the waters from the SCS, which has higher CH_4 concentrations than the wPS. As a result, the average surface CH_4 concentration in the wPS was higher than other sites of the western North Pacific.

The mean surface CH_4 concentration in the SCS was 4.5 ± 3.6 nmol L^{-1} (saturation 230%), and it was about 35% higher than that in the wPS. The SCS receives a large amount of nutrients, in the form of river discharge, atmospheric fallout, and intensive upwelling

(Chen and Huang, 1995; Chao et al., 1996). As a result, the surface water in the SCS contains more nutrients than that in the wPS (Liu et al., 2002; Chen et al., 2006). Higher nutrient contents lead to higher primary production. Although the so-called methane paradox, which concerns methanogenesis in an aerobic environment, has not yet been fully explained, substantial research indicated the possibility that biological processes are responsible for the formation of CH_4 (Traganza et al., 1979; de Angelis and Lee, 1994; Karl and Tilbrook, 1994). The riverine input brings not only nutrients into the SCS but also a high concentration of CH_4 (Chen et al., 2008a). Consequently, the surface CH_4 concentrations in the SCS were higher than those in the wPS.

The sea-to-air CH_4 flux in the wPS was 4.9 ± 4.9 μmol m^{-2} d^{-1} and in the SCS it was higher at 8.6 ± 6.4 μmol m^{-2} d^{-1}. Most areas of the SCS were probably moderate to strong sources of atmospheric CH_4, with sea-to-air flux values of 9.9 ± 8.7 μmol m^{-2} d^{-1} in the northeastern SCS, 12.0 ± 7.4 μmol m^{-2} d^{-1} in the northern SCS and the Pearl River estuary region, 8.3 ± 4.1 μmol m^{-2} d^{-1} in the southwestern SCS and 4.3 ± 3.9 μmol m^{-2} d^{-1} in the eastern and southern SCS (Table 1).

In general, the observed saturations and fluxes of CH_4 in the coastal, shelf and marginal seas varied greatly within a range of 74–10500% and 0.0095–1200 μmol m^{-2} d^{-1} (Table 2 and references therein). The observed saturations and fluxes of CH_4 in the SCS and wPS in this study fell within these ranges. On a global scale, the mean surface CH_4 concentration in the SCS is comparable to the North Aegean Sea, but higher than other areas such as the Arabian Sea, North Sea and the Yellow Sea (Table 2).

3.3. Water and CH_4 exchange between the SCS and the wPS

Since the Luzon Strait is 2200 m deep, surface and intermediate waters are exchanged unimpededly between the SCS and the wPS. Yet, waters that are deeper than 2200 m in the wPS cannot enter the SCS. Hence, waters below 2200 m in the SCS are relatively homogeneous, with hydrochemical properties similar to the water at 2200 m in the wPS (Chen et al., 2006). In the wet season, surface and intermediate waters are net-exported from the SCS to the wPS but deep water is net-imported (Chen et al., 2001). Chen et al. (2001) calculated the amount of surface water that flows out of the SCS through the Luzon Strait in the wet season as 13.9×10^6 t s^{-1} and the amount of wPS water that flows into the SCS as 12.8×10^6 t s^{-1}. Based on our data, the CH_4 concentration above 350 m in the SCS (SCS surface water layer) is 4.8 ± 5.7 nmol L^{-1}; and in the wPS (wPS surface water layer), it is 3.9 ± 1.9 nmol L^{-1} (Table 3). As a result, the net export of surface water from the SCS to the wPS carries 1.45×10^6 mol d^{-1} CH_4 in the wet season.

According to the observational data (Chen and Huang, 1996), the SCS Intermediate Water, defined by Chen and Huang (1996) as being at depths between 350 and 1350 m, is a mixture of the upwelled deep water and the surface water. The Intermediate Water flows out of the SCS at a rate of 1.8×10^6 t s^{-1} (Chao et al., 1996; Chen and Huang, 1996). As the CH_4 concentration of the SCS Intermediate Water was 3.4 ± 3.0 nmol L^{-1}, the SCS Intermediate Water exported 0.53×10^6 mol d^{-1} CH_4 to the wPS. The deep water below 1350 m flows into the SCS year-round at a rate of 1.2×10^6 t s^{-1} (Chao et al., 1996; Chen and Huang, 1996) and the CH_4 concentration was 1.5 ± 0.7 nmol L^{-1}. Consequently, the deep water from the wPS exported 0.16×10^6 mol d^{-1} CH_4 to the SCS.

Briefly, the SCS exports 1.82×10^6 mol d^{-1} CH_4 to the wPS (net value) and emits 30.1×10^6 mol d^{-1} CH_4 to the atmosphere in the wet

Table 2
Compilation of CH_4 measurements in various coastal, shelf and marginal seas.

Study area	Station	Date	Surface CH_4 (nmol L^{-1})	Saturation (%)	Sea-to-air flux (μmol m^{-2} d^{-1})	Refs.
NW Black Sea	80	Jul.–Aug. 1995	13.1 ± 10.6	173–10500	32[a]; 53[b]	Amouroux et al. (2002)
Arabian Sea	31	Feb.–Mar. 1995		173 ± 54	2.65 ± 3.73[a]	Patra et al. (1998)
	19	Jul.–Aug. 1995		200 ± 74	5.02 ± 4.59[a]	
	11	Apr.–May 1994		140 ± 37	0.032 ± 0.162[a]	
		Apr.–May 1996 Aug.–Sept. 1997	2.6–48	140–2520		Jayakumar et al. (2001)
Baltic sea	63	Feb. 1992		113 ± 5	0.0095–14.5[a]	Bange et al. (1994)
	23	Jul. 1992		395 ± 82	0.101–1200[a]	
Southern North Sea	75	Mar. 1989	2.5–43	95–1430	6–600[a]	Scranton and McShane (1991)
North Sea	117	Sept. 1992		126 ± 8	2.16 ± 1.99[a]	Bange et al. (1994)
		Aug. 1993; May 1995; Oct. 1996; Apr. 1998; Mar. 1999	2.0–67	74–2245		Upstill-Goddard et al. (2000)
Northern Bay of Bengal	14	Jan. 1994	6.42 ± 8.02		6.65 ± 7.36[b]	Berner et al. (2003)
North Aegean Sea	~5	Jul. 1993	4.80 ± 0.31	231 ± 32	1.56[a]	Bange et al. (1996)
South Aegean Sea	~30	Jul. 1993	3.17 ± 0.45	149 ± 18	1.90[a]	
Gulf of Lions (Mediterranean Sea)		Mar., June, Sept.–Nov. 1997; Jun. 1998	8–1360			Marty et al. (2001)
Yellow Sea	14	Mar.–Apr. 2001	3.43 ± 0.23	121 ± 5.4	0.81 ± 0.50[a]	Zhang et al. (2004)
East China Sea	29	Apr. 2001	3.24 ± 0.59	141 ± 23.6	1.63 ± 1.67[a] 2.77 ± 2.71[b]	Zhang et al. (2008)
	21	Sept. 2003	9.49 ± 11.00	487 ± 555	20.9 ± 54.8[a] 36.3 ± 95.7[b]	
Western Philippine Sea	68	Jul. 2004 May 2006 Jul. 2007	3.0 ± 1.2	155 ± 62	4.9 ± 4.9[c]	This study
South China Sea	122	Aug., Sept., 2003; Jul. 2004; Jul. 2005; Jul. 2006; Jul. 2007	4.5 ± 3.6	230 ± 184	8.6 ± 6.4[c]	This study

Flux estimations are follows.
[a] Liss and Merlivat (1986).
[b] Wanninkhof (1992).
[c] Wanninkhof (2014).

Table 3
CH_4 concentrations, water fluxes and CH_4 fluxes of various water masses in the SCS and wPS.

	SCS			wPS		
	Avg. Concentration nmol L^{-1}	Water Flux $\times 10^6$ t s^{-1}	CH_4 Flux $\times 10^6$ mol d^{-1}	Avg. Concentration nmol L^{-1}	Water Flux $\times 10^6$ t s^{-1}	CH_4 Flux $\times 10^6$ mol d^{-1}
Surface Water Layer (0–350 m)	4.8 ± 5.7	−13.9 ± 1.8	−5.76	3.9 ± 1.9	12.8 ± 1.1	4.31
Intermediate water Layer (350–1350 m)	3.4 ± 3.0	−1.8 ± 0.4	−0.53			
Deep Water Layer (1350–2200 m)				1.5 ± 0.7	1.2 ± 0.2	0.16

Positive and negative numbers represent inflow and outflow, respectively.

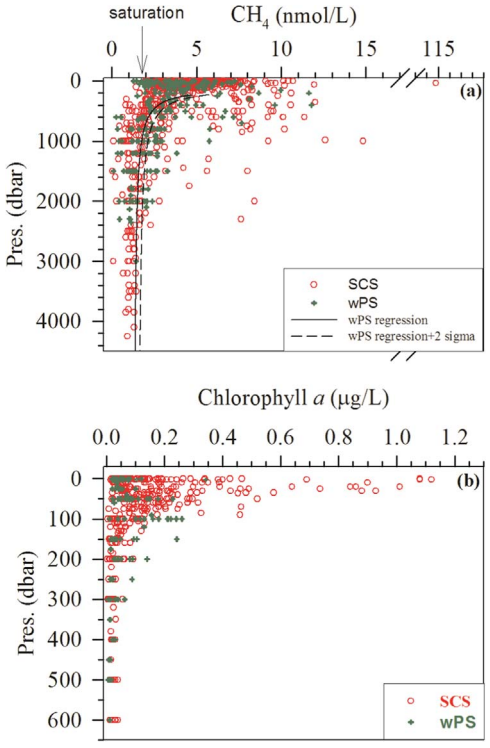

Fig. 2. Vertical distributions of (a) CH_4 (nmol L^{-1}) and (b) chlorophyll *a* (μg L^{-1}) in the western Philippine Sea, obtained at 43 stations during three cruises from July 2004 to July 2007 and in the South China Sea, obtained at 122 stations during six cruises from August 2003 to July 2007.

season. Therefore, the SCS exports CH_4 to the atmosphere and the wPS, and the SCS emits more CH_4 to the atmosphere than transports to the wPS.

3.4. Sources of CH_4 in the SCS and the wPS

3.4.1. CH_4 sources in the surface layer of the wPS

The concentrations of both CH_4 and chlorophyll *a* were high in the 150 m surface layer of the wPS (Fig. 2a and b), however, no significant correlation between CH_4 and chlorophyll *a* concentrations in the surface 150 m layer was identified herein.

Scranton and Brewer (1977) revealed the presence of a maximum CH_4 concentration above the pycnocline in the western subtropical North Atlantic. A subsurface maximum has also been widely observed in the open sea (Burke et al., 1983; Watanabe et al., 1995; Kelley and Jeffrey, 2002). In fact, the subsurface CH_4 maximum is common when examining the vertical CH_4 distribution in the water column in the open sea. Although the formation of CH_4 in the surface water layer may relate to the biological activity, and some studies (Owens et al., 1991; Damm et al., 2008; Zindler et al., 2013; Bogard et al., 2014) have indeed shown a correlation between the CH_4 and chlorophyll *a* concentrations in surface waters, no significant correlation between CH_4 and chlorophyll *a* concentrations in the surface 150 m layer was identified herein. This result not only shows that the formation of CH_4 may not be directly associated with the photosynthetic process or phytoplankton biomass, as has been suggested in some studies (Zindler et al., 2013; Bogard et al., 2014), but it also reveals that other processes, such as the physical mixing of different water masses may affect the distribution of CH_4 in the wPS.

3.4.2. CH_4 sources in the surface layer of the SCS

CH_4 maxima were observed in the subsurface layer at most stations (Fig. 2a) and the highest chlorophyll *a* concentrations throughout the water column were found above 100 m (Fig. 2b). As for the wPS, no significant correlation between CH_4 and chlorophyll *a* concentrations in the surface 100 m layer was identified.

Domain B is near the Pearl River estuary where the hydrogeochemistry is influenced by the fresh water inputs, especially in the wet season (Yin et al., 2000). Chen et al. (2008a) reported extremely high CH_4 concentrations from 23 to 2984 nmol L^{-1} in the Pearl River, its tributaries and estuary. Although the high CH_4 concentration quickly declines offshore, rivers export a large amount of CH_4 and organic matter into the coastal ocean. The riverine water brings large amounts of nutrients into the SCS (Dai et al., 2006, 2008; Chen et al., 2008a; Han et al., 2012), increasing the primary productivity and the chlorophyll *a* concentration. The river inflow caused the surface water closer to shore to have lower salinity, higher chlorophyll *a* and CH_4 concentrations (Fig. 3). In 2005, a very large amount of fresh water flowed into the SCS and greatly reduced the salinity of seawater near shore (Fig. 3d). This very large amount of the fresh water was brought by the Super-typhoon Haitang (category 5 on the hurricane scale) close to this area one week before the research cruise, causing intense precipitation and increased river discharge. Fig. 4 shows that the surface CH_4 concentration decreased with increasing salinity near the Pearl River estuary in 2005. Based on the linear equation (Fig. 4; $[CH_4] = -0.62$ salinity+26, n=19, $r^2=0.34$), when the salinity is 0, CH_4 concentration of the Pearl River in the estuary should be around 26 ± 6.9 nmol L^{-1}, which falls within the range of 6.9–173.7 nmol L^{-1} reported by Zhou et al. (2009). This result indicates that the high surface CH_4 concentration in domain B was caused by fresh water inputs, as was also reported in other areas such as the North Sea (Scranton and McShane, 1991; Rehder et al., 1998; Upstill-Goddard et al., 2000).

Domain C is in the southwestern SCS and most of it is on the Sunda Shelf. The sampling stations that were closer to the Mekong River estuary exhibited higher surface CH_4 concentrations but lower salinity comparing with other sampling stations in Domain C (Fig. 5). It revealed that although the Mekong River mouth is more than 150 km away from the sampling stations, it still affected our sampling area. According to the model simulations, the Mekong River sediment can transport to more than 250 km away from the Mekong River mouth (Xue et al., 2012). In addition, the sediment core and isotopic data showed that over the past 5500 yrs, tremendous amount of Mekong River sediment input has allowed the Mekong River Delta to prograde

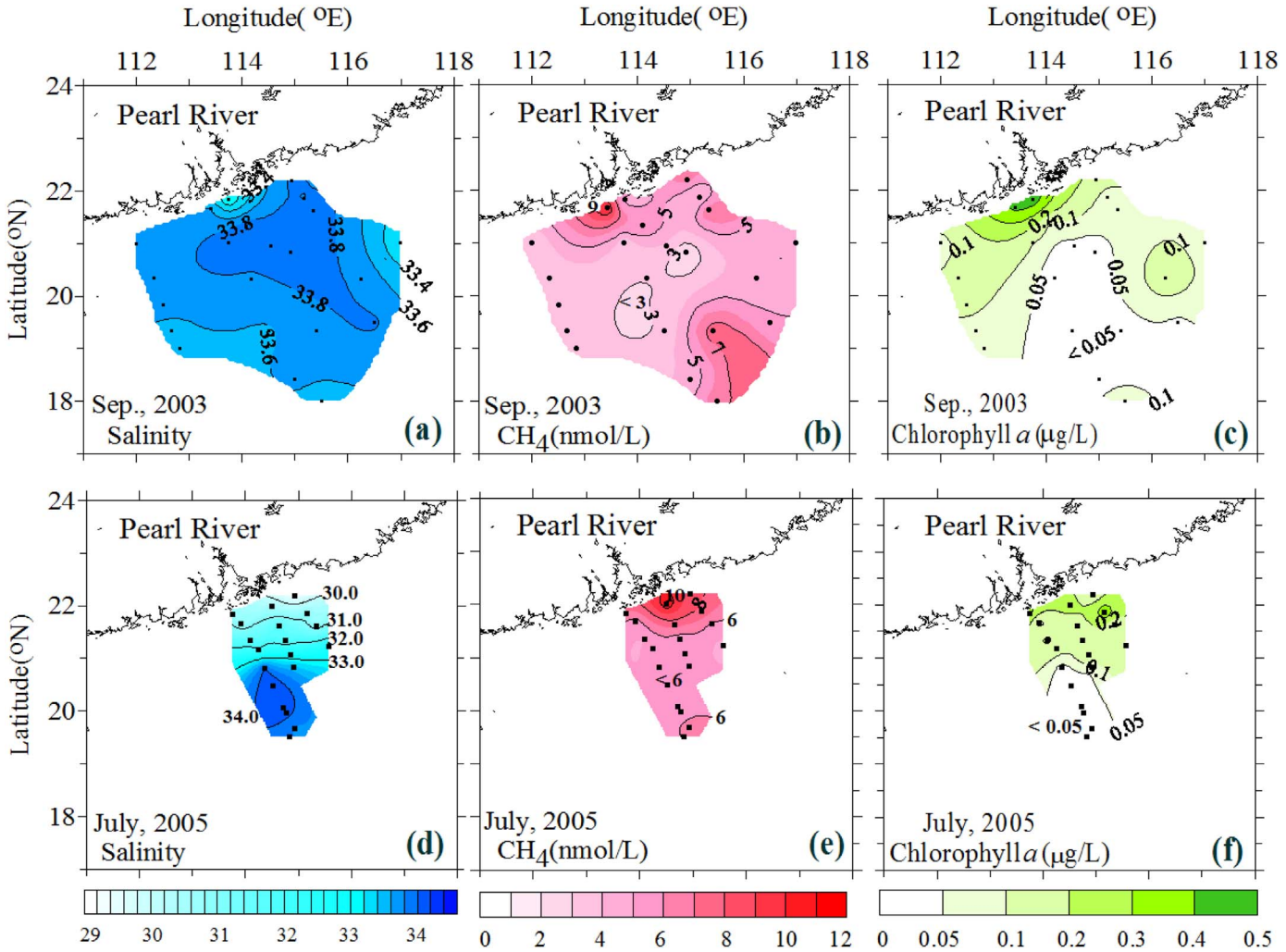

Fig. 3. Surface distributions of (a) salinity (b) CH_4 (nmol L^{-1}) and (c) chlorophyll *a* (μg L^{-1}) in September 2003; surface distributions of (d) salinity (e) CH_4 (nmol L^{-1}) and (f) chlorophyll *a* (μg L^{-1}) in July 2005 near the Pearl River estuary, obtained at 41 stations during two cruises in September 2003 and July 2005.

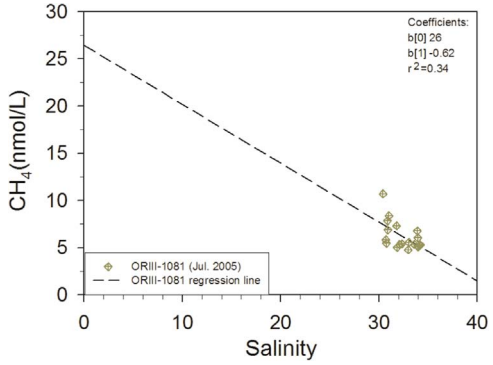

Fig. 4. Surface CH_4 (nmol L^{-1}) versus salinity near the Pearl River estuary, obtained at 19 stations during one cruise in July 2005.

more than 250 km to the southeast (Nguyen et al., 2000).

3.4.3. CH_4 sources in the intermediate and deep water layers

At most stations in the SCS and in the wPS (Fig. 2a), CH_4 concentrations generally declined with increasing depth beyond the euphotic zone and remained constant below 1,000 m. In the deep ocean, CH_4 is typically undersaturated relative to the present atmospheric mixing ratio because of lower atmospheric CH_4 concentrations at the time when deep water was formed (Rehder et al., 1999), and because of bacterial oxidation (Scranton and Brewer, 1978).

The average CH_4 concentration in the deep water layer (1350–2200 m) were 1.5 ± 0.7 nmol L^{-1} in the wPS and 1.9 ± 1.7 nmol L^{-1} in the SCS. However, there were some high CH_4 concentrations (4.2–14.8 nmol L^{-1}) at mid-depths (800–2300 m; Fig. 2a) in the SCS. High CH_4 concentrations were found in the bottom water in the area between latitude 20–22°N and longitude 118–120°E (in Domain A) and stations #19, #20 (Fig. 6; in Domain B). These signals may be related to the sediments on the upper continental slope, which are rich in organic matter and CH_4 may have been generated in the anoxic sediments. The same phenomenon has been observed in the East China Sea (ECS). For instance, Lin et al. (1992) found that the organic carbon concentrations in the bottom sediments increased across the shelf break, reaching their highest value in sediments at depths of 1000–1500 m in the ECS. Further, Zhang et al. (2008) found high concentrations of CH_4 (around 40 nmol L^{-1}) in bottom waters in the ECS, which may have been related to the production within and emission of CH_4 from the organic-rich sediments. Tseng et al. (2016) reported in the same sampling area, high N_2O concentrations which may have been produced in sediments on the continental slope.

Regions of CH_4 seepage were also discovered in Domain A with buildups of authigenic carbonate, named the Jiulong Methane Reef (Suess, 2005; Han et al., 2005, 2008). Previous research (Suess et al., 1985; Boetius et al., 2000; Boetius and Suess, 2004) has reported that the formation of authigenic carbonates at cold vent sites of continental margin has been associated with methane-rich fluid and the activity of chemosynthetic communities.

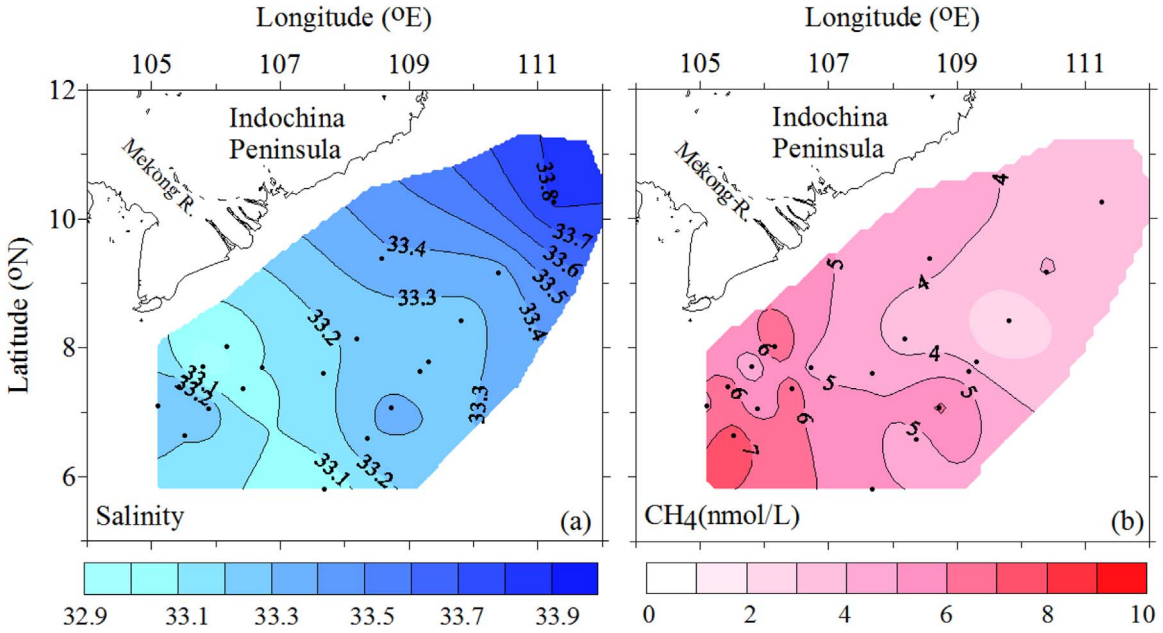

Fig. 5. Surface distributions of (a) salinity and (b) CH_4 (nmol L^{-1}) near Mekong River estuary in the South China Sea, obtained at 19 stations during one cruise in July 2006.

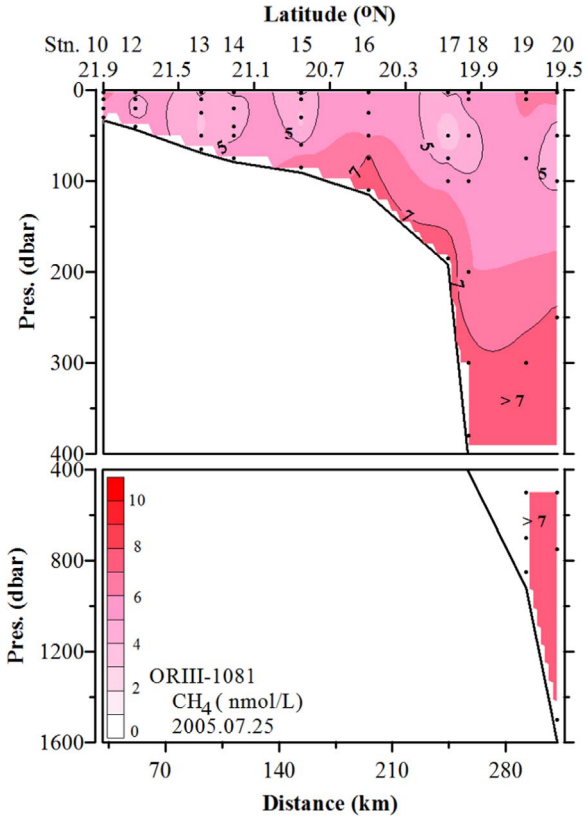

Fig. 6. Cross-section of CH_4 (nmol L^{-1}) near the Pearl River estuary, obtained at 10 stations during one cruise in July 2005.

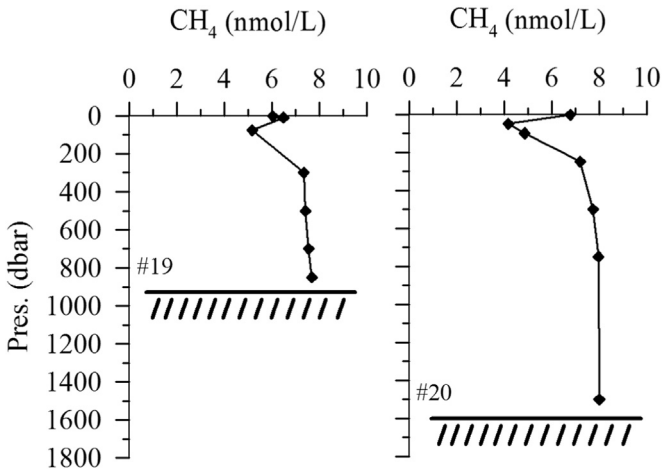

Fig. 7. Vertical distribution of the CH_4 concentrations (nmol L^{-1}) at stations #19 and #20 near the Pearl River estuary in July 2005.

The depths of sampling stations #19 (19°30.975′N; 114°49.508′E) and #20 (19° 40.427′N; 114° 55.462′E) were 850 and 1500 m, respectively. Worth mentioning is that both sampling stations had high CH_4 concentrations throughout the water column (Fig. 7), which is not common in the deep sea domain. Zhou et al. (2009) reported high bottom CH_4 concentrations (between latitude 18–20°N and longitude 113–116°E) near these two sampling stations and possibly due to CH_4 seeps from seafloor sediments. Wu et al. (2009) revealed that a large amount of hydrocarbon may be accumulated in the continental shelf of the SCS. Seismic profiles of these areas also show that bottom simulating reflectors (BSR) are widespread under the sea floor, indicative of possible gassy sediments (Wu et al., 2005). Additional geochemical evidence also suggests the presence of submarine gas hydrate deposits around these area (Chen et al., 2005; Su et al., 2005). As a result, these high mid-depth CH_4 concentrations and especially the one that was 115 nmol L^{-1} at a depth of 35 m - most likely originated from gas hydrates (Chen and Tseng, 2006) and oil gas beneath the sediment with subsequent vertical migration and advection of CH_4. The CH_4 that is released from the seafloor will migrate upward through the water column either as dissolved CH_4 or as bubbles (Zhang and Zhai, 2015).

Domain D includes the eastern and southern parts of the SCS, from the southern Luzon Strait southward along the western coast of Luzon, Palawan and Borneo. High surface CH_4 concentrations were measured along the coast of Brunei (Fig. 8a), in agreement with previous study (Rehder and Suess, 2001). The occurrence of pockmarks, indicating the recent or ancient seepage of gas or fluid from the bottom, as well as some gas seeps that have recently been active, have been identified off the shore of Brunei (Hovland and Judd, 1988). Fig. 9 presents the cross-section between the eastern and the southern SCS in 2007 (ORI-

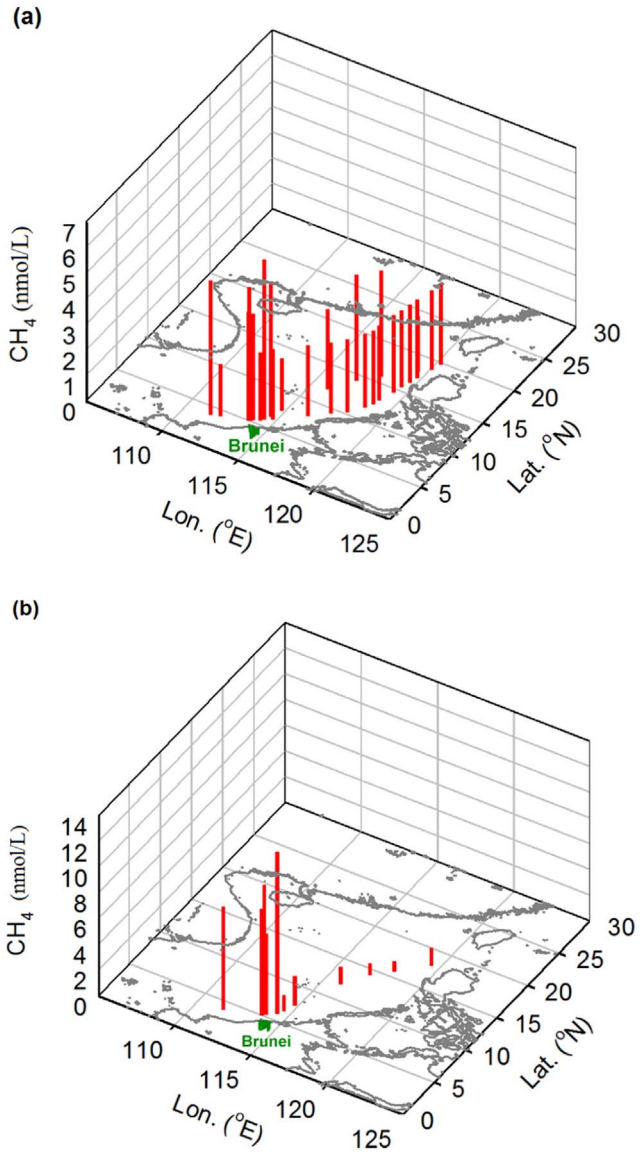

Fig. 8. Distribution of CH_4 (nmol L^{-1}) in the (a) surface water and (b) bottom water in domain D (defined in Fig. 1a) in the South China Sea, obtained at 30 stations during one cruise in July 2007.

837). The water column of the section was well stratified in both salinity and temperature during the wet season (Fig. 9a and b). But surprisingly, from sampling station SL1–SL5 (near Brunei), the CH_4 concentration did not decrease with the depth beyond euphotic zone but reaches the maxima in the bottom water (Fig. 9c). At all sampling stations near Brunei, high CH_4 concentrations were found in the bottom waters (Fig. 8b). At sampling station SL1, the CH_4 concentration reached 12.6 nmol L^{-1} in the bottom water at a depth of around 1000 m. The high CH_4 concentrations in the water column close to Brunei may reflect seepage from the abundant fossil fuel and gas deposits (OPL, 2000).

Chen and Huang (1996) and Chen et al. (2015) reported that a mid-depth boundary between 350 m and 1350 m exists near 122°E above the continental slope near the Luzon Strait. To the east of it, the water mass belongs to the wPS, whereas to the west, it is mainly the SCS water. Fig. 10 displays the CH_4 vertical distribution above 2000 m along 22°N from 121°E to 126°E. The CH_4 vertical distribution in the intermediate water along 22°N reveals rather high CH_4 concentrations west of 121.5°E. These high CH_4 concentrations in the intermediate water were presumably exported from the SCS. However, determining whether the high CH_4 concentration signals disappeared east of 121.5°E because of mixing with the wPS intermediate water, which has a lower CH_4 concentration, or because of being transferred north by the Kuroshio Current, requires further investigation.

The vertical distributions of CH_4 in the SCS and the wPS (Fig. 2a) show that many CH_4 data were higher in the SCS than in the wPS. Those higher CH_4 concentrations appeared above 2300 m in the SCS and might come from the riverine input in the surface water layer or be released from the sediment in the intermediate and deep water layers. In order to exclude the effects of sea-air exchange and the influence from the fresh water and the SCS, the correlation between CH_4 concentrations and potential temperature below 100 m in the wPS east of 121.5°E was examined (Fig. 11). The CH_4 concentrations correlate positively with potential temperature (CH_4=0.12T+1.28, n=103, r^2=0.44). As the water masses above 2200 m exchange freely between the wPS and the SCS, and waters deeper than about 2200 m originate in the 2200 m deep wPS water outside the Luzon Strait (Chen et al., 2001), the correlation of CH_4 concentrations with potential temperature in the SCS should be similar with the one in the wPS. Therefore, the values above the linear regression plus 2 sigma were likely released from the sediment in the SCS (Fig. 11).

3.5. CH_4 in the continental shelf of the SCS and future aspects

In the continental shelf and upper slope region (depth < 500 m) of the SCS, the average surface CH_4 concentration was 5.1 ± 2.1 nmol L^{-1} while at depths of greater than 500 m, it was 3.8 ± 1.6 nmol L^{-1}. Coastal regions receive more terrestrial nutrients and organic matter than deep seas, and the stronger coupling in such regions between sediments and surface waters favors high dissolved CH_4 concentrations. During the wet season, the southwesterly monsoon induces upwelling along the coastal ocean over the continental shelf of the northern SCS (Shaw, 1992; Li, 1993; Su, 1998; Gan et al., 2009) and the Vietnamese coast (Ho et al., 2000; Kuo et al., 2000; Xie et al., 2003). During the dry season, the northeasterly monsoon causes coastal upwelling off northwest Borneo Island (Yan et al., 2015), resulting in the input of nutrients. Combining CH_4 with wind speed data obtained using satellites yields estimated sea-to-air CH_4 fluxes of 11.0 ± 7.4 μmol m^{-2} d^{-1} in the continental shelf and upper slope regions, and 6.1 ± 6.0 μmol m^{-2} d^{-1} in the deep-sea regions of the SCS. The continental shelf and upper slope regions cover around 60% of the SCS area and account for approximately 72% of the CH_4 emission from the SCS.

Global warming has increased the stratification of the surface ocean, possibly expanding oxygen minimum zones (Stramma et al., 2008), and possibly increasing CH_4 production (Naqvi et al., 2010). Additionally, coastal regions are subject to increasing terrestrial inputs of nutrients and organic matter (Chen et al., 2008b; Howarth, 2008; Conley et al., 2009), and decomposition of the settled organic matter causes hypoxia when the oxygen at the bottom is insufficiently replenished. Consequently, an increasing number of coastal ecosystems are reported to exhibit hypoxia (Diaz and Rosenberg, 2008; Lui et al., 2014). Changes in nutrient and carbon exported from rivers have been demonstrated to affect exchange of biogenic trace gases, such as CO_2 (Gypens et al., 2009) and DMS (Gypens and Borges, 2014), with the atmosphere. As increasing amounts of nutrients and organic matter have been exported from the land and the hypoxic areas of coastal oceans have been increasing, more CH_4 may have accumulated in the coastal regions and more CH_4 emission may occur in the future.

4. Conclusions

In both the SCS and the wPS, CH_4 in the surface water was oversaturated with respect to the atmospheric equilibrium, and CH_4 concentrations generally declined with increasing depth below the euphotic zone, but remained constant below 1,000 m. In the SCS, some

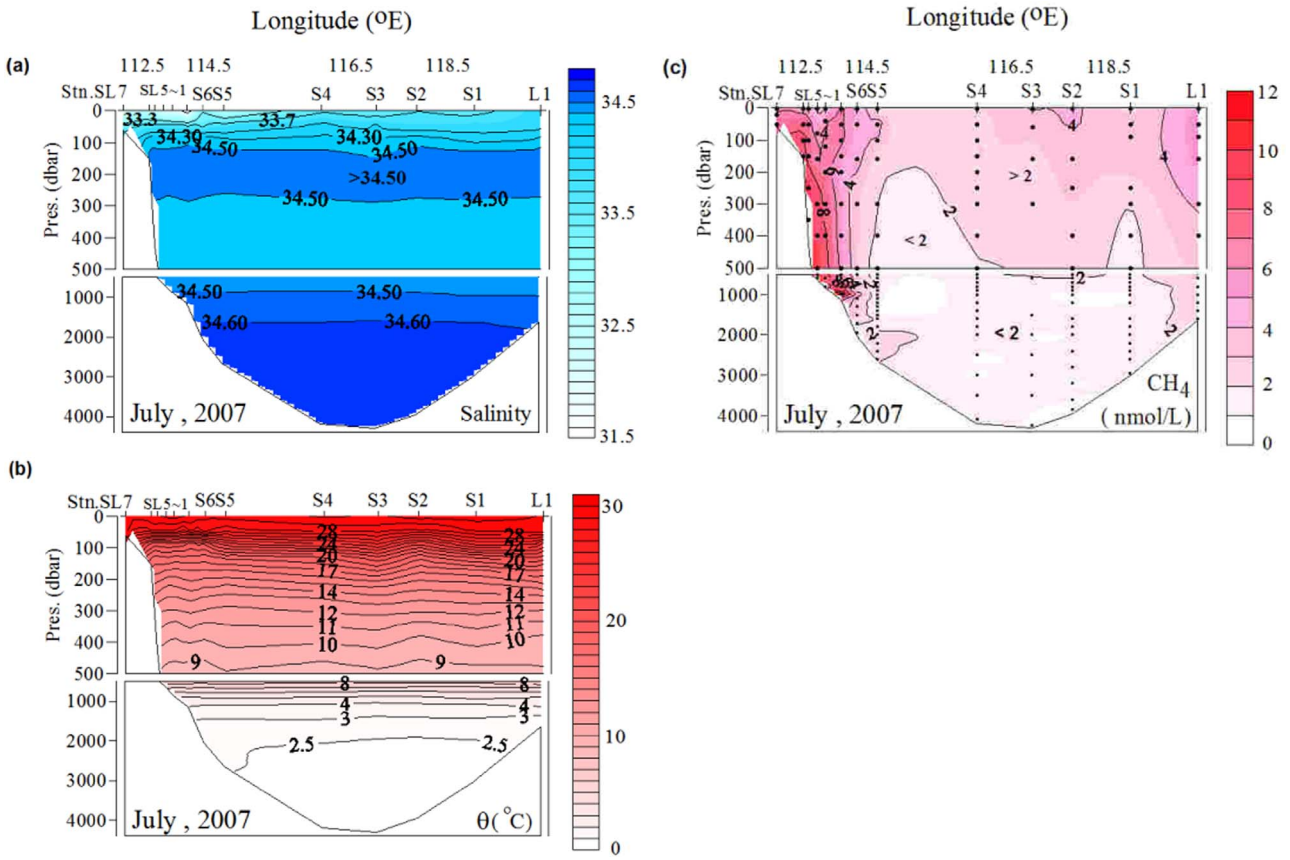

Fig. 9. Cross-section of (a) salinity; (b) potential temperature θ (°C); (c) CH_4 (nmol L^{-1}) in domain D (defined in Fig. 1a) in the South China Sea, obtained at 13 stations during one cruise in July 2007.

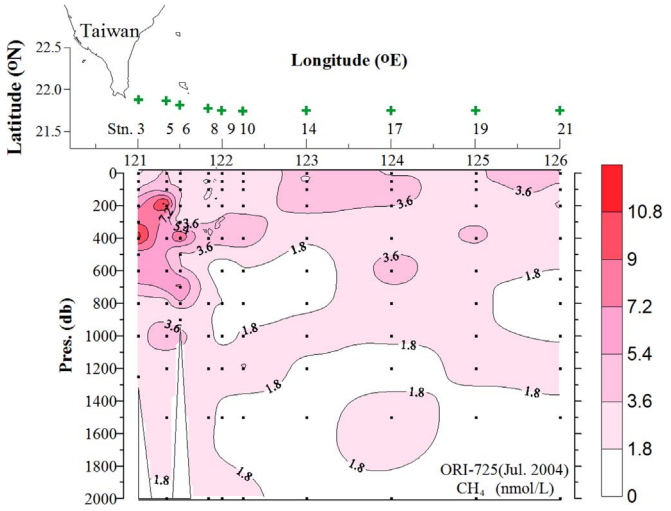

Fig. 10. Cross-section of CH_4 (nmol L^{-1}) along 22°N from 121°E to 126°E in the western Philippine Sea, obtained at 10 stations during one cruise in July 2004.

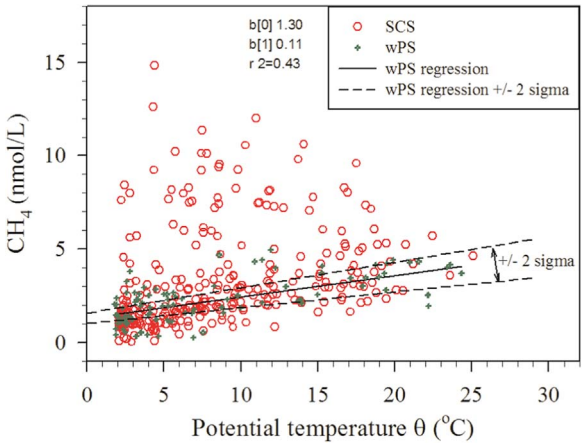

Fig. 11. The CH_4 concentration (nmol L^{-1}) versus potential temperature θ (°C) below 100 m in the South China Sea and the western Philippine Sea, obtained at 66 stations during eight cruises from August 2003 to July 2007.

high CH_4 concentrations at mid-depths were observed, and could most likely be attributed to the release of CH_4 from sediments or seepage from gas hydrates or gassy sediment.

The SCS influences the surface and intermediate waters in the wPS. This study has established that the SCS emits CH_4 to the atmosphere and also exports CH_4 to the wPS. The SCS emits more CH_4 to the atmosphere than transports to the wPS in the wet season.

The continental shelf and upper slope are responsible for approximately 72% of the emissions of CH_4 from the SCS. Since marginal seas represent a large percentage of coastal regions and are strongly affected by anthropogenic activities, the situation in marginal seas may have become more severe comparing with other sea areas. Importantly, as terrestrial input increases and coastal areas under hypoxia expand, more CH_4 may be emitted.

Acknowledgements

The authors wish to thank the Ministry of Science and Technology of the ROC, Taiwan (MOST 104-2611-M-110-015 and 104-2611-M-110-016) and the Aim for the Top University Program Project (04C030204 and 05C030204), for supporting this research, and the captains and crews of ORI and III for their assistance, and two

anonymous reviewers for constructive suggestions and comments on the previous version of the manuscript.

First author thanks the international grant from Bank Santander/ UNESCO Chair UNITWIN/WiCop and the Erasmus Mundus Programme for the MACOMA Doctoral funding contract (SGA 2012-1701/001-001-EMJD). AVB is a senior research associate at the Fonds National de la Recherche Scientifique (FNRS, Belgium).

References

Amouroux, D., Roberts, G., Rapsomanikis, S., Andreae, M.O., 2002. Biogenic gas (CH_4, N_2O, DMS) emission to the atmosphere from near-shore and shelf waters of the northwestern Black Sea. Estuar. Coast. Shelf Sci. 54, 575–587.

de Angelis, M.A., Lee, C., 1994. Methane production during zooplankton grazing on marine phytoplankton. Limnol. Oceanogr. 39, 1298–1308.

Bange, H.W., Rapsomanikis, S., Andreae, M.O., 1996. Nitrous oxide in coastal waters. Glob. Biogeochem. Cycles 10, 197–207.

Bange, H.W., Bartell, U.H., Rapsomanikis, S., Andrease, M.O., 1994. Methane in the Baltic and North Seas and a reassessment of the marine emission of methane. Glob. Biogeochem. Cycles 8, 465–480.

Berner, U., Poggenburg, J., Faber, E., Quadfasel, D., Frische, A., 2003. Methane in ocean waters of the Bay of Bengal: its sources and exchange with the atmosphere. Deep-Sea Res. II 50, 925–950.

Boetius, A., Suess, E., 2004. Hydrate ridge: a natural laboratory for the study of microbial life fueled by methane from near-surface gas hydrates. Chem. Geol. 204, 291–310.

Boetius, A., Ravenschlag, K., Schubert, C.J., Rickert, D., Widdel, F., Gieseke, A., Amann, R., Jørgensen, B.B., Witte, U., Pfannkuche, O., 2000. A marine microbial consortium apparently mediating anaerobic oxidation of methane. Nature 407, 623–626.

Bogard, M.J., del Giorgio, P.A., Boutet, L., Chaves, M.C.G., Prairie, Y.T., Merante, A., Derry, A.M., 2014. Oxic water column methanogenesis as a major component of aquatic CH_4 fluxes. Nat. Commun., 5. http://dx.doi.org/10.1038/ncomms6350.

Borges, A.V., Champenois, W., Gypens, N., Delille, B., Harlay, J., 2016. Massive marine methane emissions from near-shore shallow coastal areas. Sci. Rep. 6, 27908. http://dx.doi.org/10.1038/srep27908.

Burke, R.A., Jr., Reid, D.F., Brooks, J.M., Lavoie, D.M., 1983. Upper water column methane geochemistry in the eastern tropical North Pacific. Limnol. Oceanogr. 28, 19–32.

Cao, Z.-M., Dai, M.-H., Zheng, N., Wang, D.-L., Li, Q., Zhai, W.-D., Meng, F.-F., Gan, J.-P., 2011. Dynamics of the carbonate system in a large continental shelf system under the influence of both a river plume and coastal upwelling. J. Geophys. Res. 116, G02010. http://dx.doi.org/10.1029/2010JG001596.

Chang, H.L., Yang, S.S., 1997. Measurement of methane emission from soil. J. Chin. Agric. Chem. Soc. 35, 475–484.

Chao, S.Y., Shaw, P.T., Wu, S.Y., 1996. Deep water ventilation in the South China Sea. Deep-Sea Res. 43, 445–466.

Chen, C.T.A., Huang, M.H., 1995. Carbonate chemistry and the anthropogenic CO_2 in the South China Sea. Acta Oceanol. Sin. 14, 47–57.

Chen, C.T.A., Huang, M.H., 1996. A mid-depth front separating the South China Sea water and the West Philippine Sea water. J. Oceanogr. 52, 17–25.

Chen, C.T.A., Tseng, H.C., 2006. Abnormally high CH_4 concentrations in seawater at mid-depths on the continental slops of the northern South China Sea. Terr. Atmos. Ocean. Sci. 17, 951–959.

Chen, C.T.A., Chen, Y.S., Wang, S.L., 1994. Methane emissions from natural waters in Taiwan. Proceedings of the 7th IUAPPA Regional Conference on Air Pollution and Waste Issues, Nov. 2–4, Taipei, VI, 51–61.

Chen, C.T.A., Wang, S.L., Lu, X.X., Zhang, S.R., Lui, H.K., Tseng, H.C., Wang, B.J., Huang, H.I., 2008a. Hydrogeochemistry and greenhouse gases of the Pearl River, its estuary and beyond. Q. Int. 186, 79–90.

Chen, C.T.A., Zhai, W.D., Dai, M.H., 2008b. Riverine input and air-sea CO_2 exchanges near the Changjiang (Yangtze River) Estuary: status quo and implication on possible future changes in metabolic status. Cont. Shelf Res. 28, 1476–1482.

Chen, C.T.A., Wang, S.L., Wang, B.J., Pai, S.C., 2001. Nutrient budgets for the South China Sea basin. Mar. Chem. 75, 281–300.

Chen, C.T.A., Hou, W.P., Gamo, T., Wang, S.L., 2006. Carbonate-related parameters of subsurface waters in the West Philippine, South China and Sulu Seas. Mar. Chem. 99, 151–161.

Chen, C.T.A., Yeh, Y.T., Chen, Y.C., Huang, T.H., 2015. Seasonal and ENSO-related interannual variability of subsurface fronts separating West Philippine Sea waters from South China Sea waters near the Luzon Strait. Deep-Sea Res. I 103, 13–23.

Chen, D.F., Huang, Y.Y., Feng, D., Su, Z., 2005. Seep carbonate and preserved bacteria fossils in the northern South China Sea and their geological implications. Bull. Min. Pet. Geochem. 24, 185–189, (in Chinese).

Chuang, P.C., Yang, T.F., Lin, S., Lee, H.F., Lan, T.F., Hong, W.L., Liu, C.S., Chen, J.C., Wang, Y., 2006. Extremely high methane concentration in bottom water and cored sediments from offshore southwestern Taiwan. Terr. Atmos. Ocean. Sci. 17, 903–920.

Conley, D.J., Bj¨orck, S., Bonsdorff, E., Carstensen, J., Destouni, J., G., Gustafsson, B.G., Hietanen, S., Kortekaas, M., Kuosa, H., Meier, H.E.M., Müller-Karulis, B., Nordberg, K., Norkko, A., Nürnberg, G., Pitkänen, H., Rabalais, N.N., Rosenberg, R., Savchuk, O.P., Slomp, C.P., Voss, M., Wulff, F., Zillén, L., 2009. Hypoxia-related processes in the Baltic Sea. Environ. Sci. Technol. 43, 3412–3420.

Dai, M., Guo, X., Zhai, W., Yuan, L., Wang, B., Wang, L., Cai, P., Tang, T., Cai, W.-J., 2006. Oxygen depletion in the upper reach of the Pearl River estuary during a winter drought. Mar. Chem. 102, 159–169.

Dai, M., Zhai, W., Cai, W.-J., Callahan, J., Huang, B., Shang, S., Huang, T., Li, X., Lu, Z., Chen, W., Chen, Z., 2008. Effects of an estuarine plume-associated bloom on the carbonate system in the lower reaches of the Pearl River estuary and the coastal zone of the northern South China Sea. Cont. Shelf Res. 28 (12), 1416–1423.

Dai, M.-H., Cao, Z.-M., Guo, X.-H., Zhai, W.-D., Liu, Z.-Y., Yin, Z.-Q., Xu, Y.-P., Gan, J.-P., Hu, J.-Y., Du, C.-J., 2013. Why are some marginal seas sources of atmospheric CO_2? Geophys. Res. Lett. 40, 2154–2158. http://dx.doi.org/10.1002/grl.50390.

Damm, E., Kiene, R.P., Schwarz, J., Falck, E., Dieckmann, G., 2008. Methane cycling in Arctic shelf water and its relationship with phytoplankton biomass and DMSP. Mar. Chem. 109, 45–59.

Damm, E., Helmke, E., Thoms, S., Schauer, U., Nöthing, E., Bakker, K., Kiene, R.P., 2010. Methane production in aerobic oligotrophic surface water in the central Artic Ocean. Biogeosciences 7, 1099–1108.

Diaz, R.J., Rosenberg, R., 2008. Spreading dead zones and consequences for marine ecosystems. Science 321, 926–929.

Du, C., Liu, Z., Dai, M., Kao, S.-J., Cao, Z., Zhang, Y., Huang, T., Wang, L., Li, Y., 2013. Impact of the Kuroshio intrusion on the nutrient inventory in the upper northern South China Sea: insights from an isopycnal mixing model. Biogeosciences 10, 6419–6432. http://dx.doi.org/10.5194/bg-10-6419-2013.

Erickson, D.J., III, 1993. A stability dependant theory for air–sea gas exchange. J. Geophys. Res. 98, 8471–8488.

Florez-Leiva, L., Damm, E., Farías, L., 2013. Methane production induced by dimethylsulfide in surface water of an upwelling ecosystem. Prog. Oceanogr. 112–113, 38–48.

Forster, G., Upstill-Godard, R.C., Gist, N., Robinson, C., Uher, G., Woodward, E.M.S., 2008. Nitrous oxide and methane in the Atlantic Ocean between 50°N and 52°S: latitudinal distribution and sea-to-air flux. Deep-Sea. Res. Pt. II 56, 964–976. http://dx.doi.org/10.1016/jdsr2.2008.12.002.

Gan, J.-P., Li, L., Wang, D.-X., Guo, X.-G., 2009. Interaction of a river plume with coastal upwelling in the northeastern South China Sea. Cont. Shelf Res. 29, 728–740.

Gypens, N., Borges, A.V., 2014. Increase in dimethylsulfide (DMS) emissions due to eutrophication of coastal waters offsets their reduction due to ocean acidification. Front. Mar. Sci. 1 (4), 1–6. http://dx.doi.org/10.3389/fmars.2014.00004.

Gypens, N., Borges, A.V., Lancelot, C., 2009. Effect of eutrophication on air–sea CO_2 fluxes in the coastal Southern North Sea: a model study of the past 50 years. Glob. Change Biol. 15, 1040–1056. http://dx.doi.org/10.1111/j.1365-2486.2008.01773.x.

Han, A.-Q., Dai, M.-H., Kao, S.-J., Gan, J.-P., Li, Q., Wang, L.-F., Zhai, W.-D., Wang, L., 2012. Nutrient dynamics and biological consumption in a large continental shelf system under the influence of both a river plume and coastal upwelling. Limnol. Oceanogr. 57, 486–502.

Han, W.-Y., 1998. Marine Chemistry in the South China Sea. Science Press, Beijing, 289, (in Chinese).

Han, X., Suess, E., Huang, Y., Wu, N., Bohrmann, G., Su, X., Eisenhauer, A., Rehder, G., Fang, Y., 2008. Jiulong methane reef: microbial mediation of seep carbonates in the South China Sea. Mar. Geol. 249, 243–256.

Han, X., Suess, E., Huang, Y., Wu, N., Eisenhauer, A., Bohrmann, G., Su, X., Rehder, G., Fang, Y., shipboard scientists of Leg SO-177, 2005. Jiulong Methane reef: first direct evidence of methane seepage in the South China Sea. Geophysical Research Abstracts 7, 04055. European Geosciences Union.

Ho, C.-R., Zheng, Q., Soong, Y.S., Kuo, N.-J., Hu, J.-H., 2000. Seasonal variability of sea surface height in the South China Sea observed with TOPEX/POSEIDON altimeter data. J. Geophys. Res. 105, 13981–13990.

Hovland, M., Judd, A.J., 1988. Seabed Pockmarks and Seepages. Graham and Trotman, London, 293.

Howarth, R.W., 2008. Coastal nitrogen pollution: a review of sources and trends globally and regionally. Harmful Algae 8, 14–20.

Huang, T.H., Chen, C.T.A., Zhang, W.Z., Zhuang, X.F., 2015. Varying intensity of Kuroshio intrusion into Southeast Taiwan Strait during ENSO events. Cont. Shelf Res. 103, 79–87.

Intergovernmental Panel on Climate Change (IPCC), 2013. Working Group I Report, The Physical Science Basis. C.2; C.6; C.8, pp. 159–254; pp. 473–552; pp. 677–731.

Jayakumar, D.A., Naqvi, S.W.A., Narvekar, P.V., George, M.D., 2001. Methane in coastal and offshore waters of the Arabian Sea. Mar. Chem. 74, 1–13.

Johnson, K.M., Hughes, J.E., Donaghay, P.L., Sieburth, J.M., 1990. Bottle-calibration static head space method for the determination of methane dissolved in seawater. Anal. Chem. 62, 2408–2412.

Karl, D., Beversdorf, L., Björkman, K.M., Church, M.J., Martinez, A., DeLong, E.F., 2008. Aerobic production of methane in the sea. Nat. Geosci. 1, 473–478.

Karl, D.M., Tilbrook, B.D., 1994. Production and transport of methane in oceanic particulate organic matter. Nature 368, 732–734.

Kelley, C.A., Jeffrey, W.H., 2002. Dissolved methane concentration profiles and air–sea fluxes from 41°S to 27°N. Glob. Biogeochem. Cycles 16, 131–136.

Kirschke, S., Bousquet1, P., Ciais1, P., Saunois1, M., Canadell, J.G., Dlugokencky, E.J., Bergamaschi, P., Bergmann, D., Blake, D.R., Bruhwiler, L., Cameron-Smith, P., Castaldi, S., Chevallier, F., Feng, L., Fraser, A., Fraser1, P.J., Heimann, M., Hodson, E.L., Houweling, S., Josse, B., Krummel, P.B., Lamarque, J.-F., Langenfelds, R.L., Le Quéré, C., Naik, V., O'Doherty, S., Palmer, P.I., Pison1, I., Plummer, D., Poulter1, B., Prinn, R.G., Rigby, M., Ringeval, B., Santini, M., Schmidt, M., Shindell, D.T., Simpson, I.J., Spahni, R., Steele, L.P., Strode, S.A., Sudo, K., Szopa1, S., van der Werf, G.R., Voulgarakis, A., van Weele, M., Weiss, R.F., Williams, J.E., Zeng, G., 2013. Three decades of global methane sources and sinks. Nat. Geosci. 6, 813–823.

Kuo, N.-J., Zheng, Q., Ho, C.-R., 2000. Satellite observation of upwelling along the western coast of the South China Sea. Remote Sens.Environ. 74, 463–470.

Lamontagne, R.A., Swinnerton, J.W., Linnenbom, V.J., Smith, W.D., 1973. Methane concentrations in various marine environments. J. Geophys. Res. 78, 5317–5324.

Li, L., 1993. Summer upwelling system over the northern continental shelf of the South China Sea: a physical description. In: Su, J., Chuang, W.-S., Hsueh, R.Y. (Eds.), Proceedings of the Symposium on the Physical and Chemical Oceanography of the China Seas. China Ocean Press, Beijing, 58–68.
Lin, S., Liu, K.-K., Chen, M.-P., Chang, F.-Y., 1992. Distribution of organic carbon in the KEEP area continental margin sediments. Terr. Atmos. Ocean. Sci. 3, 365–378.
Liss, P.S., Merlivat, L., 1986. Air–sea Gas Exchange Rates: Introduction and Synthesis. The Role of Air–Sea Exchange in Geochemical Cyclings. NATO ASI Series 185. D. Reidel Publishing Company, New York, 113–127.
Liu, K.K., S.-Y. Chao, S.Y., Shaw, P.-T., Gong, G.-C., Chen, C.-C., Tang, T.Y., 2002. Monsoon-forced chlorophyll distribution and primary production in the South China Sea: observations and a numerical study. Deep-Sea Res. I 49, 1387–1412.
Lui, H.K., Chen, C.T.A., Lee, J., Bai, Y., He, X.Q., 2014. Looming hypoxia on outer shelves caused by reduced ventilation in the open oceans: case study of the East China Sea. Estuar. Coast. Shelf Sci. 151, 355–360. http://dx.doi.org/10.1016/j.ecss.2014.08.010.
Marty, D., Bonin, P., Michotey, V., Bianchi, M., 2001. Bacterial biogas production in coastal system affected by freshwater inputs. Cont. Shelf Res. 21, 2105–2115.
Morales, C.E., Anabalón, V., 2012. Phytoplankton biomass and microbial abundances during the spring upwelling season in the coastal area off Concepción, central-southern Chile: variability around a time series station. Prog. Oceanogr. 92 (1), 81–91.
Naqvi, S.W.A., Bange, H.W., Farías, L., Monteiro, P.M.S., Scranton, M.I., Zhang, J., 2010. Marine hypoxia/anoxia as a source of CH_4 and N_2O. Biogeosciences 7, 2159–2190.
Nguyen, L.V., Ta, T.K.O., Tateishi, M., 2000. Late holocene depositional environments and coastal evolution of the Mekong River Delta, Southern Vietnam. J. Asian Earth Sci. 18 (4), 427–439.
Nightingale, P.D., Malin, G., Law, C.S., Watson, A.J., Liss, P.S., Liddicoat, M.I., Boutin, J., Upstill-Goddard, R.C., 2000. In situ evaluation of air–sea gas exchange parameterizations using novel conservative and volatile tracers. Glob. Biogeochem. Cycles 14, 373–387.
OPL, 2000. South East Asia Oil & Gas Activity and Concession Map 2000 ed.. Oilfield Publications, Herefordshire.
Owens, N.J.P., Law, C.S., Mantoura, R.F.C., Burkill, P.H., Llewellyn, C.A., 1991. Methane flux to the atmosphere from the Arabian Sea. Nature 354, 293–296.
Patra, P.K., Lal, S., Venkataramani, S., Gauns, M., Sarma, V.V.S.S., 1998. Seasonal variability in distribution and fluxes of methane in the Arabian Sea. J. Geophys. Res. 103, 1167–1176.
Rehder, G., Suess, E., 2001. Methane and pCO_2 in the Kuroshio and the South China Sea during maximum summer surface temperatures. Mar. Chem. 75, 89–108.
Rehder, G., Keir, R.S., Suess, E., 1999. Methane in the northern Atlantic controlled by microbial oxidation and atmospheric history. Geophys. Res. Lett. 5, 587–590.
Rehder, G., Keir, R.S., Suess, E., Pohlmann, T., 1998. The multiple sources and patterns of methane in North Sea waters. Aquat. Geochem. 4, 403–427.
Rhee, T.S., Kettle, A.J., Andreae, M.O., 2009. Methane and nitrous oxide emissions from the ocean: a reassessment using basin-wide observations in the Atlantic. J. Geophys. Res. 114, D12304. http://dx.doi.org/10.1029/2008JD011662.
Scranton, M.I., Brewer, P.G., 1977. Occurrence of methane in the near surface waters of the western subtropical North-Atlantic. Deep-Sea Res. 24, 127–138.
Scranton, M.I., Brewer, P.G., 1978. Consumption of dissolved methane in the deep ocean. Limnol. Oceanogr. 23 (6), 1207–1213.
Scranton, M.I., McShane, K., 1991. Methane in the southern North Sea: the role of European rivers. Cont. Shelf Res. 11 (1), 37–52.
Shaw, P.T., 1992. Self circulation off the southeast coast of China. Rev. Aquat. Sci. 6 (1), 1–28.
Sheu, W.-J., Wu, C.-R., Oey, L.-Y., 2010. Blocking and westward passage of eddies in the Luzon Strait. Deep-Sea Res. II. http://dx.doi.org/10.1016/j.dsr2.2010.04.004.
Stramma, L., Johnson, G.C., Sprintall, J., Mohrholz, V., 2008. Expanding oxygen-minimum zones in the tropical oceans. Science 320, 655–658.
Strickland, J.D.H., Parsons, T.R., 1972. A Practical Handbook of Seawater Analysis. Fisheries Research Board of Canada, Ottawa, Canada, 310.
Su, C.Y., Niu, B.H., Wang, H.Y., Zhao, K.B., 2005. A study of gas hydrate geochemical exploration and deposit formation patterns in the Xisha ocean. Earth Sci. Front. 12, 243–251, (in Chinese).
Su, J., 1998. Circulation dynamics of the China seas north of 18°N. In: Allan, R.R., Kenneth, H., Brink (Eds.), The Sea, Vol. 11, The Global Coastal Ocean: Regional Studies and Syntheses. Wiley, NY, 483–505.
Suess, E., 2005. RV SONNE cruise report SO 177, Sino–German cooperative project, South China Sea Continental Margin: geological methane budget and environmental effects of methane emissions and gashydrates. IFM-GEOMAR Reports. ⟨http://store.pangaea.de/documentation/Reports/SO177.pdf⟩.
Suess, E., Carson, B., Ritger, S., Moore, J.C., Jones, M., Kulm, L.D., Cochrane, G., 1985. Biological communities at vent sites along the subduction zones off Oregon. In: Jones, M.L. (ed), The hydrothermal vents of the Eastern Pacific: An Overview. Bull Biol Soc Wash, 6, 475–484.
Traganza, E.D., Swinnerton, J.W., Cheek, C.H., 1979. Methane supersaturation and ATP-zooplankton blooms in near-surface waters of the Mediterranean and the subtropical North Atlantic Ocean. Deep-Sea Res. 26, 1237–1245.
Tseng, H.C., Chen, C.T.A., Borges, A.V., DelValls, T.A., Lai, C.M., Chen, T.Y., 2016. Distributions and sea-to-air fluxes of nitrous oxide in the South China Sea and the West Philippines Sea. Deep-Sea Res. I 115, 131–144.
Upstill-Goddard, R.C., Barnes, J., Frost, T., Punshon, S., Owens, N.J.P., 2000. Methane in the southern North Sea: low-salinity inputs, estuarine, and atmospheric flux. Glob. Biogeochem. Cycles 14, 1205–1216.
Wanninkhof, R., 1992. Relationship between wind speed and gas exchange over the ocean. J. Geophys. Res. 97 (C5), 7373–7382.
Wanninkhof, R., 2014. Relationship between wind speed and gas exchange over the ocean revisited. Limnol. Oceanogr.: Methods 12, 351–362.
Watanabe, S., Higashitani, N., Tsurushima, N., Tsunogai, S., 1995. Methane in the western North Pacific. J. Oceanogr. 51, 39–60.
Wiesenburg, D.A., Guinasso, N.L., Jr, 1979. Equilibrium solubilities of methane, carbon monoxide, and hydrogen in water and seawater. J. Chem. Eng. Data 24, 356–360.
Wu, S.G., Zhang, G.X., Huang, Y.Y., 2005. Gas hydrate occurrence on the continental slope of the northern South China Sea. Mar. Petrol. Geol. 22, 403–412.
Wu, S.G., Sun, Q.L., Wu, T.Y., Yuan, S.Q., Ma, Y.B., Yao, G.S., 2009. Polygonal fault and oil–gas accumulation in deep-water area of Qiongdongnan Basin. Acta Pet. Sin. 30, 22–32, (in Chinese).
Xie, S.-P., Xie, Q., Wang, D., Liu, W.T., 2003. Summer upwelling in the South China Sea and its role in regional climate variations. J. Geophys. Res. 108 (C8), 3261. http://dx.doi.org/10.1029/2003JC001867.
Xue, Z., He, R., Liu, J.P., Warner, J.C., 2012. Modeling transport and deposition of the Mekong River sediment. Cont. Shelf Res. 37, 66–78.
Yan, Y., Ling, Z., Chen, C., 2015. Winter coastal upwelling off northwest Borneo in the South China Sea. Acta Oceanol. Sin. 34, 3–10.
Yang, T.F., Chuang, P.C., Lin, S., Chen, J.C., Wang, Y., Chung, S.H., 2006. Methane venting in gas hydrate potential area offshore of SW Taiwan: evidence of gas analysis of water column samples. Terr. Atmos. Ocean. Sci. 17, 933–950.
Yin, K., Qian, P., Chen, Jv.C., Hsieh, D.P.H., Harrison, P.J., 2000. Dynamics of nutrients and phytoplankton biomass in the Pearl River estuary and adjacent waters of Hong Kong during summer: preliminary evidence for phosphorus and silicon limitation. Mar. Ecol.: Prog. Ser. 194, 295–305.
Yuan, Y., Liao, G., Yang, C., 2008. The Kuroshio near the Luzon Strait and Circulation in the Northern South China Sea during August and September 1994. J. Oceanogr. 64, 777–788. http://dx.doi.org/10.1007/s10872-008-0065-6.
Zhang, G., Zhang, J., Ren, J., Li, J., Liu, S., 2008. Distributions and sea-to-air fluxes of methane and nitrous oxide in the North East China Sea in summer. Mar. Chem. 110, 42–55.
Zhang, G.L., Zhang, J., Kang, Y.B., Liu, S.M., 2004. Distributions and fluxes of dissolved methane in the East China Sea and the Yellow Sea in spring. J. Geophys. Res. 109 (C7), C07011. http://dx.doi.org/10.1029/2004JC002268.
Zhang, Y., Zhai, W.-D., 2015. Shallow-ocean methane leakage and degassing to the atmosphere: triggered by offshore oil-gas and methane hydrate explorations. Front. Mar. Sci. 2, 34. http://dx.doi.org/10.3389/fmars.2015.00034.
Zhou, H., Yin, X., Yang, Q., Wang, H., Wu, Z., Bao, S., 2009. Distribution, source and flux of methane in the western Pearl River Estuary and northern South China Sea. Mar. Chem. 117, 21–31.
Zindler, C., Bracher, A., Marandino, C.A., Taylor, B., Torrecilla, E., Kock1, A., Bange, H.W., 2013. Sulphur compounds, methane, and phytoplankton: interactions along a north–south transit in the western Pacific Ocean. Biogeosciences 10, 3297–3311.